(2)

OFFICE OF NAVAL RESEARCH

Contract N00014-84-G-0201

AD-A240 148

Task No. 0051-865

Technical Report #42

# Surface Electrochemistry of Chloro(phthalocyaninato)rhodium(III) Species, and Oxygen Reduction Electrocatalysis, Formation of a Dimeric Species

By

Y.-H. Tse, P. Seymour, N. Kobayashi, H. Lam, C.C. Leznoff, and A.B.P. Lever*

in

Inorganic Chemistry

York University
Department of Chemistry, 4700 Keele St., North York
Ontario, Canada M3J 1P3

Reproduction in whole, or in part, is permitted for any purpose of the United States Government

*This document has been approved for public release and sale; its distribution is unlimited

*This statement should also appear in Item 10 of the Document Control Data-DD form 1473. Copies of the form available from cognizant contract administrator

91 3 3 090

91-09496

SECURITY CLASSIFICATION OF THIS PAGE

# REPORT DOCUMENTATION PAGE

| | |
|---|---|
| 1a. REPORT SECURITY CLASSIFICATION | 1b. RESTRICTIVE MARKINGS |
| 2a. SECURITY CLASSIFICATION AUTHORITY<br>Unclassified | 3. DISTRIBUTION/AVAILABILITY OF REPORT<br>As it appears on the report |
| 2b. DECLASSIFICATION/DOWNGRADING SCHEDULE | |
| 4. PERFORMING ORGANIZATION REPORT NUMBER(S)<br>Report # 42 | 5. MONITORING ORGANIZATION REPORT NUMBER(S) |
| 6a. NAME OF PERFORMING ORGANIZATION<br>A.B.P. Lever, York University<br>Chemistry Department<br>6b. OFFICE SYMBOL (If applicable) | 7a. NAME OF MONITORING ORGANIZATION<br>Office of Naval Research |
| 6c. ADDRESS (City, State, and ZIP Code)<br>4700 Keele St., North York, Ontario M3J 1P3<br>Canada | 7b. ADDRESS (City, State, and ZIP Code)<br>Chemistry Division<br>800 N. Quincy Street<br>Arlington, VA 22217 U.S.A. |
| 8a. NAME OF FUNDING/SPONSORING ORGANIZATION<br>8b. OFFICE SYMBOL (If applicable) | 9. PROCUREMENT INSTRUMENT IDENTIFICATION NUMBER<br>N00014-84-G-0201 |
| 8c. ADDRESS (City, State, and ZIP Code) | 10. SOURCE OF FUNDING NUMBERS<br>PROGRAM ELEMENT NO. / PROJECT NO. / TASK NO / WORK UNIT ACCESSION NO |

11. TITLE (Include Security Classification)
Surface Electrochemistry of Chloro(phthalocyaninato)rhodium(III) Species, and Oxygen Reduction Electrocatalysis, Formation of a Dimeric Species

12. PERSONAL AUTHOR(S)
Y.-H. Tse, P. Seymour, N. Kobayashi, H. Lam, C.C. Leznoff, and A.B.P. Lever*

| 13a. TYPE OF REPORT | 13b. TIME COVERED | 14. DATE OF REPORT (Year, Month, Day) | 15. PAGE COUNT |
|---|---|---|---|
| Technical | FROM Aug. '90 TO Aug. '91 | August 20, 1991 | 33 |

16. SUPPLEMENTARY NOTATION

| 17. COSATI CODES | | |
|---|---|---|
| FIELD | GROUP | SUB-GROUP |
| | | |
| | | |

18. SUBJECT TERMS (Continue on reverse if necessary and identify by block number)
Rhodium, Phthalocyanine, Surface Electrochemistry, Dimer

19. ABSTRACT (Continue on reverse if necessary and identify by block number)

The deposition of Chloro(phthalocyaninato)rhodium(III) onto a highly oriented pyrolytic graphite (HOPG) electrode leads to a surface which can be organized by polarizing to potentials negative of the reduction of rhodium(III) to rhodium(II). The organized surface contains dinuclear rhodium phthalocyanine which is fairly stable in its $[Rh^{II}Pc]_2$ oxidation state. It is reversibly oxidized to a $[Rh^{III}Pc]_2$ dinuclear species which decomposes slowly to monomeric $Rh^{III}Pc$ detected upon the surface through its electroactivity. Reduction of this mononuclear $Rh^{III}Pc$ back to $Rh^{II}Pc$ leads to redimerization. The surface electrochemistry of this dynamic interplay between mononuclear and dinuclear species is explored in depth. The dinuclear $[Rh^{II}Pc]_2$ species reacts with oxygen to form oxygen adducts which appear to be involved in both the 2-electron reduction of oxygen to hydrogen peroxide, and the 4-electron reduction to water. However these two processes proved difficult to characterize.

| | |
|---|---|
| 20. DISTRIBUTION/AVAILABILITY OF ABSTRACT<br>☒ UNCLASSIFIED/UNLIMITED ☐ SAME AS RPT ☐ DTIC USERS | 21. ABSTRACT SECURITY CLASSIFICATION<br>Unclassified/unlimited |
| 22a. NAME OF RESPONSIBLE INDIVIDUAL<br>Dr. Ronald A. De Marco | 22b. TELEPHONE (Include Area Code) / 22c. OFFICE SYMBOL |

DD FORM 1473, 84 MAR — 83 APR edition may be used until exhausted. All other editions are obsolete.

SECURITY CLASSIFICATION OF THIS PAGE

## TECHNICAL REPORT DISTRIBUTION LIST - GENERAL

Office of Naval Research (2)*
Chemistry Division, Code 1113
800 North Quincy Street
Arlington, Virginia 22217-5000

Dr. James S. Murday (1)
Chemistry Division, Code 6100
Naval Research Laboratory
Washington, D.C. 20375-5000

Dr. Robert Green, Director (1)
Chemistry Division, Code 385
Naval Weapons Center
China Lake, CA 93555-6001

Dr. Eugene C. Fischer (1)
Code 2840
David Taylor Research Center
Annapolis, MD 21402-5067

Dr. Elek Lindner (1)
Naval Ocean Systems Center
Code 52
San Diego, CA 92152-5000

Commanding Officer (1)
Naval Weapons Support Center
Dr. Bernard E. Douda
Crane, Indiana 47522-5050

Dr. Richard W. Drisko (1)
Naval Civil Engineering
Laboratory
Code L52
Port Hueneme, CA 93043

Dr. Harold H. Singerman (1)
David Taylor Research Center
Code 283
Annapolis, MD 21402-5067

Chief of Naval Research (1)
Special Assistant for Marine
Corps Matters
Code 00MC
800 North Quincy Street
Arlington, VA 22217-5000

Defense Technical Information
Center (2)
Building 5, Cameron Station
Alexandria, VA 22314

DTIC
COPY
INSPECTED
2

Accession For
NTIS GRA&I
DTIC TAB
Unannounced
Justification
By
Distribution/
Availability Codes
Avail and/or
Dist Special
A-1

* Number of copies to forward



Enclosure (2)

# ABSTRACT DISTRIBUTION LIST

Professor Hector Abruña
Department of Chemistry
Cornell University
Ithaca, NY 14853

Professor C. A. Angell
Arizona State University
Department of Chemistry
Tempe, AZ 85287

Professor Allen Bard
Department of Chemistry
University of Texas at Austin
Austin, TX 78712-1167

Professor Douglas Bennion
Department of Chemical Engineering
350 CB
Birgham Young University
Provo, UT 84602

Professor Lesser Blum
Department of Physics
University of Puerto Rico
Rio Piedras, PUERTO RICO 00931

Professor Daniel Buttry
Department of Chemistry
University of Wyoming
Laramie, WY 82071

Professor Bruce Dunn
Departement of Materials Science and Engineering
University of California, Los Angeles
Los Angeles, CA 90024

Professor Andrew Ewing
Department of Chemistry
152 Davey Laboratory
Pennsylvania State University
University Park, PA 16802

Professor Gregory Farrington
University of Pennsylvania
Department of Materials Science and Engineering
3231 Walnut Street
Philadelphia, Pennsylvania 19104

Professor W. R. Fawcett
Department of Chemistry
University of California, Davis
Davis, CA 95616

Professor Harry Gray
California Institute of Technology
127-72
Pasadena, California 91125

Professor Joel Harris
Department of Chemistry
University of Utah
Salt Lake City, UT 84112

Professor Adam Heller
Department of Chemical Engineering
University of Texas at Austin
Austin, TX 78712-1062

Professor Pat Hendra
The University
Southampton SO9 5NH
ENGLAND

Professor Joseph Hupp
Department of Chemistry
Northwestern University
Evanston, IL 60208

Professor Jiri Janata
Department of Bioengineering
University of Utah
Salt Lake City, UT 84102

Professor A. B. P. Lever
Department of Chemistry
York University
4700 Keele Street
North York, Ontario M3J 1P3

Professor Nathan S. Lewis
Division of Chemistry and Chemical Engineering
California Institute of Technology
Pasadena, CA 91125

Professor Rudolph Marcus
Division of Chemistry and Chemical Engineering
California Institute of Technology
Pasadena, CA 91125

Professor Charles Martin
Department of Chemistry
Colorado State University
Ft. Collins, CO 80523

Professor Royce W. Murray
Department of Chemistry
University of North Carolina at Chapel Hill
Chapel Hill, NC 27514

Dr. Michael R. Philpott
IBM Research Division
Almaden Research Center
650 Harry Road
San Jose, CA 95120-6099

Professor B. S. Pons
Department of Chemistry
University of Utah
Salt Lake City, UT 84112

Dr. Debra Rolison
Code 6170
Naval Research Laboratory
Washington, DC 20375-5000

Professor Donald Schleich
Department of Chemistry
Polytechnic University
333 Jay Street
Brooklyn, NY 11201

Professor Jack Simons
Department of Chemistry
University of Utah
Salt Lake City, UT 84112

Dr. H. Gilbert Smith
TSI Mason Research Institute
57 Union Street
Worcester, MA 01608

Professor Eric Stuve
Department of Chemical Engineering, BF-10
University of Washington
Seattle, WA 98195

Dr. Stanislaw Szpak
Code 634
Naval Ocean Systems Center
San Diego, CA 92152-5000

Professor Petr Vanýsek
Department of Chemistry
Northern Illinois University
Dekalb, IL 60115

Professor Michael Weaver
Department of Chemistry
Purdue University
West Lafayette, IN 49707

Professor Henry White
Department of Chem. Eng. and
Materials Science
421 Washington Ave., SE
University of Minnesota
Minneapolis, MN 55455

Professor. Mark Wightman
Department of Chemistry
University of North Carolina
Chapel Hill, NC 27599-1350

Professor George Wilson
Department of Chemistry
University of Kansas
Lawrence, KS 66045

Professor Mark S. Wrighton
Department of Chemistry
Massachusetts Institute of Technology
Cambridge, MA 02139

Professor Ernest Yeager
Case Center for Electrochemical Sciences
Case Western Reserve University
Cleveland, OH 44106

12741

# Surface Electrochemistry of Chloro(phthalocyaninato)rhodium(III) Species, and Oxygen Reduction Electrocatalysis. Formation of a Dimeric Species.

Yu-Hong Tse, Penny Seymour, Nagao Kobayashi,[1] Herman Lam, Clifford C. Leznoff, and A.B.P.Lever*

**Abstract**

The deposition of Chloro(phthalocyaninato)rhodium(III) onto a highly oriented pyrolytic graphite (HOPG) electrode leads to a surface which can be organized by polarizing to potentials negative of the reduction of rhodium(III) to rhodium(II). The organized surface contains dinuclear rhodium phthalocyanine which is fairly stable in its $[Rh^{II}Pc]_2$ oxidation state. It is reversibly oxidized to a $[Rh^{III}Pc]_2$ dinuclear species which decomposes slowly to $^{III}Pc$ detected upon the surface through its electroactivity. Reduction of this mononuclear $Rh^{III}Pc$ back to $Rh^{II}Pc$ leads to re-dimerization. The surface electrochemistry of this dynamic interplay between mononuclear and dinuclear species is explored in depth. The dinuclear $[Rh^{II}Pc]_2$ species reacts with oxygen to form oxygen adducts which appear to be involved in both the 2-electron reduction of oxygen to hydrogen peroxide, and the 4-electron reduction to water. However these two processes proved difficult to characterize.

## Introduction

Many cobalt and iron $MN_4$ macrocyclic complexes catalyze the electroreduction of oxygen.[2-8] Most mononuclear cobalt macrocycles catalyze the 2-electron reduction to hydrogen peroxide, but some dinuclear cobalt complexes catalyze the much more desirable 4-electron reduction to water in strongly acidic[9,10] or basic[11] media. Iron porphyrins[2-8] and a dinuclear iridium porphyrin,[12] generally catalyze the 4-electron process. Among the phthalocyanines, the iron[13-16] and platinum[17] species are active, in alkaline media, in the 4-electron reduction of oxygen. There are reports of a catena-CN-bridged Co(III)Pc[18] and a mononuclear long chain ring substituted Co(II) phthalocyanine[19] being active in the four-electron reduction of oxygen. However there is no detailed understanding of the role of pH nor indeed of the structural design aspects which favor the 4-electron process over the 2-electron process.

Although the cobalt macrocycles catalyze the 2-electron reduction of oxygen, the existence of the iridium species catalyzing the direct 4-electron process raises the question of whether rhodium macrocycles would be capable of 4-electron reduction, either in a mononuclear form analogous to iron phthalocyanine, or in a dinuclear form analogous to the iridium porphyrin.[12] We describe here results obtained with chlororhodium(III) phthalocyanine (1)[20,21] adsorbed on highly oriented pyrolytic graphite (HOPG). Evidence for both a 2-electron and a 4-electron reduction process was obtained, but we were unsuccessful in determining precisely the conditions which would favor one mechanism over the other.

Nevertheless, in pursuing this investigation, some very interesting surface electrochemical characteristics were observed. The weakly aggregated species attach to the electrode in an irregular fashion giving a poorly organized surface. Reduction to $Rh^{II}$ phthalocyanine leads to a dimerization process and electrochemically cycling the electrode converts the poorly organized surface into a simple surface containing almost solely a dimeric rhodium phthalocyanine species.

This paper reports the stability, redox chemistry and oxygen reduction chemistry of this dimer surface.

## Experimental

Materials: Tetrabutylammonium perchlorate (TBAP, Aldrich) recrystallized from absolute ethanol was dried in a vacuum oven at 50°C for 48 hours. 1,2-Dichlorobenzene (DCB, Aldrich) and dimethylformamide (DMF, Aldrich) were used as supplied. Argon gas (Linde) was purified by passage through heated copper filings, anhydrous $CaSO_4$ (Drierite), molecular sieves (BDH 3A), and glass wool. Oxygen gas (Linde) was used as received.

Buffer solutions were prepared from 0.1 M solutions of reagent grade $H_3PO_4$, $KH_2PO_4$, $K_2HPO_4$ and KOH, and adjusted to the desired pH, and approximately constant ionic strength. Distilled water for buffer solutions was doubly distilled in glass from alkaline $KMnO_4$, then passed through a Barnstead organic removal cartridge and two Barnstead mixed resin ultrapure cartridges. Buffer solutions were saturated with argon or oxygen for about 1 hour, and maintained under an atmosphere of the appropriate [illegible] ng data collection. Oxygenated solutions contained an oxygen concentration of approximately $10^{-3}$ M.

Physical measurements: Electronic spectra were recorded with a Hitachi Perkin-Elmer Model 340 microprocessor spectrometer or a Guided Wave Inc. Model 100-20 optical waveguide spectrum analyzer with a WW100 fiber optic probe. FTIR spectra were obtained as Nujol mulls using a Nicolet SX20 instrument.

Solution electrochemical data were obtained with a Princeton Applied Research (PARC) model 174 potentiostat, or a PARC model 173 polarographic analyzer, coupled to a PARC model 175 universal programmer. Cyclic voltammetry and differential pulse voltammetry (DPV) carried out under an atmosphere of argon, used a conventional three electrode cell. The working electrode, described by the cross-sectional area of a 27-gauge platinum wire (area $10^{-3}$ $cm^2$), was sealed in glass. A platinum wire also served as the counter electrode. The reference electrode was a silver wire quasi-electrode separated from the working compartment by a glass frit. The potentials were referenced internally to the ferricenium/ferrocene (Fc+/Fc) couple (+0.40 V vs SCE, in DMF).

Electrochemical studies of the surface species were performed with a Pine Instrument RDE-3 potentiostat and the rotating studies with a Pine Instrument PIR rotator. The working electrode material for both surface electrochemical and oxygen reduction studies was highly oriented pyrolytic graphite (HOPG) having a circular area of 0.495 $cm^2$. Before each experiment, the HOPG electrode surface was cleaned by removing several layers of the surface with a transparent adhesive tape. For the adsorption of the catalysts onto the HOPG surface, the electrode was immersed in a 1-5 x $10^{-5}$ M phthalocyanine solution in DCB, containing about 5% ethanol, for ca. 15 minutes, removed from the solution and washed with ethanol and distilled water. The cell comprized a separate chamber for each electrode, with a Luggin capillary extending from the reference chamber to the proximity of the HOPG surface. For the aqueous experiments, an SCE and a large platinum plate were used as a reference and a counter electrode, respectively. For collection of rigorously oxygen-free data, the catalyst adsorption and its study was undertaken with equipment inside a Vacuum Atmospheres Controlled Atmosphere Box.

A bulk solution containing the dimeric $[Rh^{II}Pc]_2$ was prepared by polarizing a DMF solution of $ClRh^{III}Pc$ (2 x $10^{-4}$ M; 0.2 M TBAP) at -0.9 V vs AgCl/Ag for 3 Hr. This solution, maintained in a Vacuum Atmospheres drybox, was used to deposit the dimeric species directly upon a prepared HOPG electrode; deposition time 0.5 - 1.0 Hr.

<u>Chloro(phthalocyaninato)rhodium(III)</u> (1) ($ClRh^{III}Pc$)

The $ClRh^{III}Pc$ was prepared from $RhCl_3.2H_2O$, phthalonitrile and urea, using the melt method[22]. The melt solidified after 15 minutes' heating over an open flame, and was cooled to ambient temperature, whereupon the fused solid was broken down by boiling with ethanol. The ethanol was boiled off, and the solid crude $ClRh^{III}Pc$ (plus unreacted starting materials and impurities) extracted with benzene for 41 hours, then extracted with acetone for 48 hours, and with pyridine for 2 hours. The solid recovered from the pyridine extract was further extracted with $CH_2Cl_2$ for some 15-20 hours, then dissolved in DMF and poured into cold dilute HCl. The resulting precipitate was subsequently boiled with 1 M HCl, filtered and washed with 0.1 M HCl, and finally dried <u>in vacuo</u> at 100°C for 7 hours. Anal: Found C 58.72; H 2.70; N 17.09. Calc. C

59.05; H 2.47; N 17.21% FTIR: 1523s, 1502m, 1331m, 1287m, 1169m, 1122s, 1066m, 913m, 777w, 757m, 729s, 574w $cm^{-1}$. uv/vis ($\lambda_{max}$ nm (log $\epsilon$)) 342 (4.45), 598 (4.46), 665 (5.15), in DCB. Similar data for $ClRh^{III}Pc$ dissolved in chloroform have been reported.[20]

Chloro(tetraneopentoxyphthalocyaninato)rhodium(III) (**2**) (ClRhTNPc)

4-Neopentoxyphthalonitrile (1.28 g, 6 mmol) and $Rh_2(CO)_2Cl_2$ (0.25 g, 0.75 mmol) were heated in N,N'-dimethylaminoethanol (25 mL) at 165°C for 48 h. The crude reaction mixture was poured into water, filtered, washed and dried overnight to yield 1.5 g of crude green solid. This solid was pre-absorbed onto flash silica gel and eluted with 1:1 hexane/chloroform to give, upon evaporation, a bluish-green solid. Yield (0.12 g, 7 %) of dark blue shining crystals. Anal. Found for ClRhTNPc.Hexane C,64.6; H, 6.0; N, 10.0. Calcd. C,64.41; H, 6.52; N, 10.36% FTIR 2955s, 2868s, 1611s, 1508m, 1488m, 1457w, 1397s, 1385s, 1285w, 1237s, 1129s, 1111s, 1061s, 1013m, 826w, 753w $cm^{-1}$. These data are very similar to those reported for a series of divalent MTNPc derivatives.[23] Uv/vis ($\lambda_{max}$ nm (log $\epsilon$)) 349(4.48), 594(4.43), 657(5.21), in DCB.

## Results

i) Solution electrochemistry: The cyclic voltammogram of $ClRh^{III}Pc$ in DMF solution (Figure 1) shows three major features: a reversible couple, **A**, at +0.05 V vs SCE, two widely-separated peaks at -0.15 V (anodic), **B**, and -0.65 V (cathodic), **C**, and another reversible couple, **D**, near -1.4 V vs. SCE. The couples **A** and **B** were generated only by polarizing the electrode negative of peak **C**. If the solution is cooled to about -72°C, peak **C** becomes reversible, peak **B** disappears and peak **A** is replaced by a small irreversible anodic peak at 0.32 V. A spectroelectrochemical study of the bulk reduced species obtained by reduction some 100 mV negative of peak **C**, produces the spectra shown in Figure 2. The solution electrochemistry has been studied as a function of solvent, temperature and supporting electrolyte. The salient features are reported in the Discussion section, but the details will appear elsewhere.[24]

ii) Surface electrochemistry: **Drybox or argon conditions**: It is necessary to distinguish carefully two sets of conditions used for studying the surface electrochemistry. In one set, drybox conditions were used to exclude all traces of oxygen. In the other set, an argon-degassed cell was

employed in the open laboratory to obtain the initial "oxygen-free" conditions prior to saturating the cell with oxygen to study oxygen electrocatalysis. These "oxygen-free" conditions in degassed argon do in fact contain traces of oxygen which it proved impossible to absolutely exclude without using a controlled atmosphere box (drybox).

We have studied both the unsubstituted phthalocyanine species ClRh(III)Pc, (**1**), and ClRh(III)TNPc, (**2**), (TNPc = tetraneopentoxyphthalocyanine, being a mixture of isomers having one neopentoxy group in a peripheral position in each of the benzene rings). The results are described for both systems without differentiation except where such distinction is relevant.

In both the drybox and open laboratory experiments, the first scan cyclic voltammogram of a freshly prepared chlororhodium phthalocyanine-modified HOPG electrode run negatively from about 0.3 V shows no peak near 0 V, but does have rapidly rising cathodic current more negative than about -0.5 V (for (**1**), and more negative than about -0.6 V for (**2**)) with a more prominent peak at about -0.9 - (-1.0) V, for species (**1**), and nearer -0.8 V for species (**2**) (labelled peak **V** below) (Figure 3 A,B). If this scan is extended, negatively, beyond the peak at about -0.8 V, and then switched, there is a decline in the cathodic current in the -0.5 - (-1.0) V region, a dramatic loss of current in peak **V**, and the build up of a new reversible peak near 0 V (peak **I**) ( + 0.03 V for ClRhPc, and -0.05 V vs SCE, for ClRhTNPc, at pH 12.9), during the second and subsequent scans. Peak **I** builds up rapidly if multiple scans are switched near -1.0 - (-1.2) V. It is just barely observable if a freshly deposited surface is switched at -0.6 V. Such scans reach an equilibrium when the current of peak **I** ceases to increase with subsequent scans. Species (**1**) and (**2**) behave analogously except that equilibrium formation of peak **I** is much more facile for species (**2**), being almost complete by the second scan (Figure 3A).

Peak **I** is most clearly observed in basic medium. As the pH decreases, the half-peak potential for couple **I** shifts positive with a slope of -34 (±3) mV/pH unit (species **1**), (Table 1) the current decreases, and, at pH less than about 8, the features lose both resolution and intensity. Most studies were carried out at pH 12.9, to which the following results and discussion refer.

Under argon, in the open laboratory conditions, three additional weak peaks are generally

seen, at -0.25 - (-0.33) V (peak **II**, cathodic), -0.5 V (peak **III**) and -0.78 (Peak **IV**, cathodic) (Figure 3B). Their relative currents vary somewhat from experiment to experiment. Peaks **II** and **IV** are generally irreversible showing no anodic counterpart, while peak **III** usually has an anodic counterpart at the same potential.

The current of peak **II** increases relative to that of peak **I** with decreasing concentration of the deposition DCB solution (Figure 3C) (equilibrium conditions). The electronic spectrum of the $ClRh^{III}Pc$/DCB solution does not obey Beer's Law, with formation of aggregated species[25] being evident at concentrations as low as $1 \times 10^{-4}$ M. Thus deposition from more concentrated solutions likely deposits aggregated rather than monomeric species on the surface.

Under drybox, oxygen-free, conditions, in these equilibrium scans, peak **II** may appear weakly and reversible, while peaks **III** and **IV** are very weak or indeed absent (Figure 3C).

<u>iii) Stability of peak I</u> (Expts. with $ClRh^{III}TNPc$ (**2**)) : The species giving rise to peak **I** is, as demonstrated below, a surface-bound dimeric rhodium tetraneopentoxyphthalocyanine which is not completely stable on the surface. If, after the equilibrium scan is established, the cyclic voltammogram is switched some 150 mV either side of peak **I**, i.e. scanning repeatedly over peak **I**, the peak collapses over a few cycles and disappears, even though there are no other apparent redox processes within 150 mV of peak **I**. Thus the surface-bound dimeric $[RhTNPc]_2$ is unstable upon polarizing over peak **I**.

To determine whether it is the $Rh^{II}TNPc$ dimer (**3**), and/or $Rh^{III}TNPc$ dimer, (**4**), which is unstable, an equilibrium scan was first established, and then the potential held constant, 150 mV <u>negative</u> of peak **I** (i.e. with $Rh^{II}TNPc$ dimer, (**3**), on the surface) for 5 minutes. A DPV scan then showed a decrease in the cathodic current of peak **I** of some 40%. Similarly if an equilibrium surface is held just <u>positive</u> of peak **I** for only 0.5 minutes, and then a DPV scan run, the cathodic DPV current is reduced by 70%. Thus decomposition of the oxidized dimer $[Rh^{III}TNPc]_2$ (**4**), (which probably has bound hydroxide ions in the outer axial sites, i.e. is really $(HO)Rh^{III}TNPc.TNPcRh^{III}(OH)$) is fairly rapid, but decomposition of the $[Rh^{II}TNPc]_2$ species, (**3**), is relatively slow.

Consistent with this observation, the anodic charge for peak **I** is always slightly greater than the cathodic charge. This is because there is some loss of dimeric species every time the electrode is polarized positive of the anodic component.

If a surface, having been cycled over the potential corresponding to peak **I** is now polarized to negative potentials, then increased reduction current is seen in the range -0.3 - (-0.5) V (Figure 4c). Further, if the surface of (**2**) is polarized at 0 V for 30 s (Figure 4a,b), resulting in a loss of 70% of the charge of peak **I**, and is then polarized to -0.5 V and switched, 90% of the initial charge is recovered (Figure 4c,d).

It is interesting to observe that with a brand new surface showing a strong peak **V**, it is necessary to cycle beyond -0.8 - (-1.0) V (beyond peak **V**) before there is significant growth of peak **I**. However when an equilibrium surface with peak **I** has been produced and then polarized beyond 0 V, to cause loss of current intensity in peak **I**, it is only necessary to polarize the electrode to about -0.5 V to recover couple **I**.

Further, if a surface is polarized between about +0.2 V and -1.0 V, then, as the scan rate is decreased and the amount of time the surface remains as $[Rh^{III}TNPc]_2$ increases, the charge under peak **II** increases, at the expense of the charge under peak **I**. Data for this experiment are analyzed in Figure 5, as follows. Assume that at the highest scan rate, 150 mV/s, there is negligible decomposition of the dimer since it exists as $[Rh^{III}TNPc]_2$ (**4**) for a very short period. Then, considering first the current, a line drawn between this 150 mV/s datum point, and zero, provides the theoretical dependence of current upon scan rate, for no decomposition (recall that current is proportional to scan rate for a surface bound species).[26] Then, observe that at lower scan rates the experimental points for peak **I** lie below the calculated line for no decomposition while those for peak **II** lie above it. Similarly, the charge under peak **II** is proportionately larger, at low scan rates, than at high scan rates, while the reverse is true for peak **I**. These charges reflect direct measurements of the ratio of "standing population" of the species responsible for peaks **I** and **II** and show that the dimeric species, decomposes when polarized positive of peak **I**, to form the species displaying peak **II**. The total charge under these two peaks is constant as is necessary (Figure 5b).

While, in principle, kinetic data could be extracted from this experiment, the uncertainty as to the residual (charging) current would lead to rather large errors in the data shown in Figure 5. The result is illustrative of the experiment undertaken and provides useful insight into surface behavior, but does not merit further analysis.

Note that the dimeric $[Rh^{III}Pc]_2$ species prepared from $ClRh^{III}Pc$, or directly from the bulk dimer solution (vide infra), is very much more stable than the corresponding $[Rh^{III}TNPc]_2$ perhaps because the neopentoxy groups in the latter species interfere with the stabilization of the dimer. Cycling over peak I for $[RhPc]_2$ (± 300 mV, 100 mV/s) leads to a loss of some 50% of the current only after about 10 minutes.

<u>iv) Surface Deposition from a Bulk Dimer Solution:</u> Bulk electrolysis of a solution of $ClRh^{III}Pc$ in DMF at potentials negative of peak C (Figure 1) yields solutions whose electronic spectra (Figure 2) are consistent with the formation of the $[Rh^{II}Pc]_2$ dimeric species.

When an electrode is dipped into this solution for 0.5 - 1 hr, a dimer surface is directly laid down. In contrast to the voltammetry discussed above, this pre-made dimer surface exhibits peak I on the first scan, and exhibits no rapidly rising cathodic current negative of -0.5 V on the first scan.

There appear to be two slightly different dimer species on the surface, differing perhaps in their axially bound counter ion or solvent. As initially formed in the fashion described above, one species exhibits an anodic peak at 0.15 V and its cathodic counterpart at 0.13 V vs SCE. In addition there is an cathodic peak for the second species observed at 0.02 V vs SCE (with no anodic partner). If the surface is held for about 15 minutes, polarized at about 0.3 V, then subsequent scans reveal only one dimer peak couple at 0.02 V identical to within experimental error, with the species reported in section (ii) above.

Thus deposition from the bulk dimer solution leads, after polarization of the resulting surface at 0.3 V, to the same surface as that generated from the bulk monomer solution.

<u>v) Introduction of oxygen</u>: Considering the data in Figure 6. The initial equilibrium surface (Figure 6a) is exposed to 0.01 mM oxygen and polarized around peak I. There is a fairly rapid loss

of signal for peak **I** (Figure 6b). If this same surface, in the 0.01 mM oxygenated solution, is polarized out to -1.0 V, a new diffusion (cathodic) peak (as indicated by scan rate dependence) designated peak **II($O_2$)** is seen at the same potential as peak **II**. Further, and most significantly, peak **I** is restored essentially quantitatively, but with the anodic component notably larger than the cathodic component. A similar experiment under a saturated oxygen environment (1 mM $O_2$) gave essentially the same results. Even under saturated oxygen conditions, scanning beyond -0.5 V regenerates peak **I**, though with somewhat less charge than the initial argon surface. The loss of peak **I** when polarizing is limited to ± 150 mV of peak **I** centre, under a saturated oxygen environment, is more rapid than when cycling is undertaken under argon.

The peak potential for peak **II($O_2$)** (in the presence of 0.01 mM $O_2$) shifts negatively about 45 mV with change in scan rate from 12.5 to 150 mV/s, (species **1**) consistent with a relatively slow rate constant for oxygen reduction. When the aqueous buffer solution is saturated with oxygen (ca. 1.1 mM)[27], a typical voltammogram for oxygen reduction on MPc/HOPG is obtained (Figure 7A), with $E_p$ = -0.4 V vs. SCE (at pH = 13) and a peak current of about 300 - 400 $\mu$A. The $O_2$ reduction peak potential is a function of pH, as expected[15,19] shifting to more positive potentials with lower pH; however because of the variability of the surface, peak potential data versus pH were somewhat scattered and are not further discussed.

**RDE Experiments under an oxygen atmosphere**: Figure 7B shows data collected with a rotating HOPG disk, using the $ClRh^{III}Pc$-modified equilibrium surface shown in Figure 3B. Using the Levich equation[28], the number of electrons, **n**, involved in the reduction was 2.1-2.2, indicating a 2-electron reduction from oxygen to hydrogen peroxide.

However, if a surface was deliberately exposed to a small amount of oxygen during cycling to equilibrium, then upon subsequent exposure to saturated oxygen, the rotating disk study led to n > 3 electrons, though this was not invariably true.

The deliberate addition of some deoxygenated hydrogen peroxide to an argon equilibrium surface yielded an increase in the current of the anodic component of peak **I** showing re-oxidation of hydrogen peroxide at that potential.

## Discussion:

**Solution electrochemistry**: Kadish and co-workers have reported[29] an electrochemical study of the analogous ClRhTPP species (TPP = tetraphenylporphyrin). The results for $ClRh^{III}Pc$ are very similar to those for ClRhTPP as is immediately evident by comparing the solution voltammogram for $ClRh^{III}Pc$ shown in Figure 1, with the corresponding data for ClRhTPP (Figure 1, ref.29).

On the basis of the ClRhTPP analysis, and detailed experiments on $ClRh^{III}Pc$ to be reported elsewhere,[24] the following conclusions concerning the solution voltammogram shown in Figure 1 can be drawn.

A bulk solution of $ClRh^{III}Pc$, in DMF, reduced at peak **C** forms a $Rh^{II}$ derivative which, at ambient temperature, immediately dimerizes forming a species $[Rh^{II}Pc]_2$ whose identity as a dimeric species is supported through spectroelectrochemical measurements. (Figure 2), and analogy with the corresponding formation of a dimeric species upon reduction of ClRhTPP.[29]

This dimerization is suppressed at - 72°C when a reversible monomeric $Rh^{III}/Rh^{II}$ redox process is observed, at -0.82 V. Peak **D**, at -1.42 V, represents the further reduction of this dimer species.

Peaks **A** and **B** are not observed unless the scan proceeds beyond a potential corresponding with peak **C**, and thus are dimer oxidation processes. These dimer re-oxidation peaks **A,B** are missing in the -72°C experiment because the dimer is not present under these conditions. Peak **A** is a reversible two-electron oxidation to form $[Rh^{III}Pc]_2^{2+}$ (with charge likely compensated by supporting electrolyte anions). Peak B is evidently associated with the formation of the dimeric species but its identity is not clear.[31]

**Surface electrochemistry**: (Oxygen-free conditions) Peak **I** appears at essentially the same potential as observed for the two-electron dimer redox process $[Rh^{III}Pc]_2/[Rh^{II}Pc]_2$ in solution, and the shift with pH is consistent with a two-electron process. Further, this peak is the only peak observed (between +0.5 V and -1.0 V vs SCE) when deposition is carried out with bulk $[Rh^{II}Pc]_2$ dimer solution. Therefore peak **I** is a two-electron $Rh^{III}/Rh^{II}$ couple for a dimeric $[RhPc]_2$

species, see Scheme I.

The surface voltammetry can be understood in terms of the following model. When freshly laid down, the $ClRh^{III}Pc$ gathers in randomly distributed, poorly organized and likely aggregated species, interacting fairly weakly with the electrode surface. Assumptions have been made[30] that, on highly-oriented pyrolytic graphite, phthalocyanines will adsorb by interaction of the macrocycle **pi**-clouds with those of the graphite lattice, and thus that the macrocycle lies flat on the graphite. However, simple microscopic examination of a supposedly "mirror" graphite surface shows many imperfections which can act as nucleating sites for the catalyst. Formation of "clumps" on the electrode surface will be further facilitated if the catalyst is already aggregated.

These poorly organized species give rise to the reduction current seen in the initial voltammogram between -0.5 and -1.0 V, and especially to peak **V** near -0.8 - (-0.9) V (Figures 3A,C). This potential corresponds to that observed -0.82 V) for the quasi-reversible mononuclear $ClRh^{III}Pc/Rh^{II}Pc$ process in DMF/TBAP at -72°C[24] and is similarly assigned here to reduction of $ClRh^{III}Pc$ to $Rh^{II}Pc$. Because of the close association of the $Rh^{II}Pc$ species in these aggregates, the $Rh^{II}Pc$ fragments rapidly dimerize giving rise to peak **I**, and hence peak **V** is irreversible.

The species $[Rh^{II}Pc]_2$ (**3**) is somewhat unstable when oxidized to the rhodium(III) dimer, $[Rh^{III}Pc]_2^{2+}$ (**4**), splitting apart slowly into mononuclear $Rh^{III}$ phthalocyanine fragments, (**5**). When cycling is carried out around 0 V, the resulting $[Rh^{III}Pc]^+$ fragments (**5**) are not reduced and therefore cannot re-dimerize, and couple **I** collapses completely. However when such a surface is polarized more negatively, then current is increased in the region beyond about -0.35 V (Figure 4c) because of the reduction of these $Rh^{III}$ phthalocyanine fragments, (**5**), to mononuclear $Rh^{II}Pc$, (**6**) which rapidly re-dimerize so that when cycling is extended negative of the potential corresponding to peak **II**, the dimer couple, **I**, is restored essentially quantitatively (see Figures 4c,d). Thus peak **II** is associated with the $Rh^{III}/Rh^{II}$ couple of a mononuclear rhodium phthalocyanine species.

The rhodium(II) dimeric species (**3**) decomposes slowly on the surface. It is probable that,

in fact, this species is intrinsically stable on the surface, as it is in solution, but that it is slowly converted to mononuclear species by reaction with trace oxygen or other reactive impurities. The amount of material on the surface of the electrode is of the order of 40 femtomoles so that very little reactive impurity is needed to destroy it.

Consideration of the charge under the dimer peak **I**, and assuming a two-electron process, gave a coverage (over a series of experiments) in the range of 20 - 40% of a monolayer of dimers; we only very rarely observed greater coverage than this. Under drybox conditions, the very weak peak **II** corresponds to about 0.5% surface coverage. Thus a lot of the surface apparently remains uncovered. The apparent reversibility of peak **II** under drybox conditions may then arise through mononuclear $Rh^{II}Pc$ (**6**) species which are too far apart to dimerize.

Peak **II** at -0.35 - (-0.45) V, associated with the reduction of mononuclear $Rh^{III}Pc$, is positive of the corresponding peak in solution at -0.82 V [low temperature reversible datum]. Therefore surface-bound mononuclear rhodium phthalocyanine, (**6**), is stabilized in the divalent state relative to the solution species[31] probably because of the interaction of the odd electron in the $d_{z^2}$ orbital, with the graphite surface, i.e. the rhodium(II) is probably bound chemically to the surface. A fresh surface containing poorly organized $ClRh^{III}Pc$ which is not, in its reduced $Rh^{II}Pc$ state, chemically bound to the graphite surface will show a redox potential near -0.8 V (peak **V**).

Dimerization of the $Rh^{II}Pc$ species (slowly upon cycling with $ClRh^{III}Pc$ (**1**), and rapidly with ClRhTNPc (**2**)) organizes the surface such that peak (**V**) is lost. Once formed, this bound dinuclear $[Rh^{II}Pc]_2$ (**3**) oxidizes at a potential positive of peak (**I**), to $[Rh^{III}Pc]_2$ (**4**) which when it subsequently decomposes to mononuclear (**5**), remains bound to the graphite surface, albeit perhaps weakly. This $[Rh^{III}Pc]^+$ species (**5**), then, can be reduced in the range -0.25 - (-0.4) V, peak **II**, to produce $Rh^{II}Pc$ (**6**) bound to the graphite surface; this can readily dimerize. The spread of potentials likely reflects possible alternate axial ligands including water, supporting electrolyte anion, and oxygen (vide infra). Indeed the more negative potential of peak **V**, relative to peak **II**, in the initial scan is partially a consequence of the bound chloride ion which is lost during reduction to $Rh^{II}Pc$, and which would stabilize rhodium(III). The possibility that the axial bound chlo-

ride ion is the primary reason for the difference in these potentials and that binding to the graphite surface is not a factor, seems improbable on the basis that the addition of chloride ion (0.1 M) to the electrolyte solution (pH 12.9) does not cause peak **V** to be retained beyond the first scan.

Peak **IV** is seen weakly on some equilibrium surfaces, but does not always occur. It was frequently (but not always) absent from the drybox collected data suggest that it might be assigned to another oxygen adduct, or perhaps the $\mu$-oxygen bridged species $PcRh^{III}ORh^{III}Pc$. $\mu$-Oxo bridged phthalocyanines and porphyrins have reduction potentials significantly negative of the corresponding process in the mononuclear species;[32] thus the observation of peak **IV** negative of peak **II** is consistent with this assignment.

<u>Surface electrochemistry under oxygen</u>: Peak **II($O_2$)** is clearly an oxygen reduction peak occurring at the same potential as the $Rh^{III}Pc/Rh^{II}Pc$ monomeric couple (peak **II** under argon) (Figure 6). The increase in current in the anodic component of peak **I** is due to hydrogen peroxide reoxidation occurring at a potential the same as that of the dimer species oxidation and corresponding roughly with the thermodynamic oxidation potential at pH 12.9. Some catalytic reoxidation of hydrogen peroxide may be involved.[33]

Dimer species $[Rh^{II}Pc]_2$ (3) reacts with oxygen, but slowly, because:-

a) peak **I** is diminished but not lost in the presence of a low level of oxygen (Figure 6),

b) cycling just negative of peak **I**, under oxygen, causes a faster collapse of peak **I**, than cycling under argon,

c) peak **I** can be regenerated if the oxygenated surface is polarized more negative than peak **II($O_2$)**, (ca -0.5 V) (Figure 4)

d) cathodic oxygen reduction occurs some 200 - 350 mV negative of couple **I** (Figure 6).

Note that during a positive ongoing scan while the potential is in the range from about -0.2 V (positive of peak **II**) to 0 V (negative of peak **I**) $[Rh^{II}Pc]_2$ (3) will exist on the surface and will be oxidized by oxygen. If such oxidation were very rapid, peak **I** would disappear; instead it is diminished relative to the situation under an argon atmosphere situation. If one were to argue that only mononuclear, and not dinuclear, rhodium phthalocyanine surface species react with oxygen, then

the magnitude of peak **I** should be independent of whether the atmosphere is argon or oxygen.

Dimeric rhodium(II) porphyrins react with oxygen to form both monomeric superoxorhodium(III) and bridged dinuclear peroxorhodium(III) porphyrin species[34-38]. Iridium octaethylporphyrin is also believed to form a $\mu$-peroxo dimeric species[12]. Therefore analogous species, viz $(O_2)Rh^{III}Pc$ (**7**) and $PcRh^{III}O_2Rh^{III}Pc$ (**8**), are also likely found on the phthalocyanine surface. It has also previously been demonstrated[38] that $(O_2)Rh^{III}TPP$ is irreversibly reduced, to a dimeric $[Rh^{II}TPP]_2$ species, at a potential slightly less negative than that of $(Cl)(Me_2NH)Rh^{III}TPP$; thus oxygenated rhodium(III) phthalocyanine may be reduced at a potential close to that of some unoxygenated mononuclear rhodium(III) phthalocyanine species.

During the cycling to equilibrium in the argon experiment where trace oxygen is probably present, some of the rhodium species will be trapped as oxygen adducts. The increased current near -0.25 - (-0.4) V, (peak **II** under argon, Figure 3B) then arises from a superimposition of a) reduction of $Rh^{III}Pc$ monomer species (**5**) generated through decomposition of (**4**), b) the reduction of oxygen adducts, (**7**) and/or (**8**), plus c) some very small current due to reduction of diffusing trace oxygen. Peak **III**, which is usually absent in data collected under drybox conditions likely arises from an oxygen adduct differing from that responsible for current near peak **II**.

The oxygen reduction process occurring at peak **II** may be represented by a series of reactions:-

$$[Rh^{II}Pc]_2 + 2\,O_2 \text{ ------> } 2\,[(O_2^-)Rh^{III}Pc] \qquad (1)$$

$$[(O_2^-)Rh^{III}Pc] + 2e^- + H^+ \text{ ---> } HO_2^- + [Rh^{II}Pc] \qquad (2)$$

$$2\,[Rh^{II}Pc] \text{ ---> } [Rh^{II}Pc]_2 \qquad (3)$$

where the oxygen adduct is assumed to be mononuclear (**7**), but might readily be dinuclear (**8**), without effecting the overall argument. The recovery of peak **I** upon scanning under oxygen negatively of -0.5 V is explained through equations (2) and (3), i.e. the reduced oxygen adduct will immediately redimerize, cf. the RhTPP system.[38]

RDE experiments yield higher n values if the initial surface has some contact with oxygen, than if it does not. The formation of an equilibrium surface in the presence of a small amount of

oxygen, followed by the oxygen electrocatalysis study, might yield a different distribution of oxygen adducts on the surface, than if the initial surface is generated oxygen-free. One might then speculate that mononuclear (**7**) acts as a 2-electron reductant to hydrogen peroxide, while dinuclear (**8**) acts as a 4-electron reductant to water. However it has proved very difficult to control these surfaces to routinely obtain n values in excess of 3 electrons.

**Summary**

The processes seen on the rhodium phthalocyanine modified HOPG electrode may be summarized (also see Scheme I):-

Peak **I**: Reversible dimeric RhPc species redox, (**3**) < = = = > (**4**)

Peak **II**: Mononuclear RhPc species redox, (**5**) < = = = > (**6**).

Peak **II**($O_2$): Reduction of diffusing oxygen possibly via a $Rh^{III}Pc$ oxygen adduct species.

Peak **III**: Oxygen adduct redox process.

Peak **IV**: Possible reduction of $PcRh^{III}ORh^{III}Pc$.

Peak **V**: Reduction of disorganized $ClRh^{III}Pc$ species.

The rhodium phthalocyanine surface has turned out to offer some unusual behavior with the dynamic interplay between mononuclear and dinuclear species on the surface being especially noteworthy. By appropriate control of the polarization potential it would clearly be possible to "hold" any one of several different RhPc species on the surface. Our initial objective to demonstrate a 4-electron reduction pathway for oxygen met with only limited success. However the chemistry developed offers some important future avenues, such as the possibility that these equilibria can be coupled to other multi-electron electrocatalytic processes, in addition to that with oxygen.

Acknowledgements

We are indebted to Drs. K. Kandil, and K. Jayaraj, for experimental assistance, to Dr. Pawel Janda for useful discussions, and the Natural Sciences and Engineering Research Council (Ottawa) and the Office of Naval Research (Washington) for financial assistance. Our thanks are also expressed to Johnson-Matthey for the loan of $RhCl_3$, and to Union Carbide for the HOPG.

Figure Legends

Figure 1. Solution electrochemical cyclic voltammogram for $ClRh^{III}Pc$, (**1**), in DMF (0.1 M TBAP). Platinum working electrode. Scan rate 100 mV/s. In all CV scans reported in these Figures, cathodic current (reduction) is uppermost.

Figure 2. Spectroelectrochemical study of the reduction of $ClRh^{III}Pc$ (**1**) in dimethylformamide. For details see text.

Figure 3A. Cyclic voltammograms for ClRhTNPc, (**2**), on HOPG in 0.1 M KOH, scan rate 100 mV/s, drybox condition. a) first scan after adsorption, positive ongoing from 0 V.; b) second scan after adsorption ; c) equilibrium scan. The potentials and surface charges of the various peaks are as follows: (peak, V, $\mu C/cm^2$) I, -0.05, 3.01; II, -0.35, 0.81; IV, -0.80, 0.16; V, -0.75, 8.38. The potentials remain constant from one experiment to another but surface charges vary. Charges reported here and in subsequent Figures are typical, and are rather approximate given the uncertainty in assessing the charging current.

Figure 3B. Cyclic voltammogram for $ClRh^{III}Pc$ (**1**) on HOPG in 0.1 M KOH, scan rate 100 mV/s, argon degased. a) first scan after adsorption, positive ongoing from 0 V.; b) equilibrium scan. The potentials and surface charges of the various peaks are as follows: (peak, V, $\mu C/cm^2$) I, 0.03, 1.41; II, -0.32, 0.48; III, -0.48, 0.63; IV, -0.72, 0.15; V, -0.96, 8.8.

Figure 3C. Cyclic voltammograms for $ClRh^{III}Pc$ (**1**) in 0.1 M KOH, scan rate 100 mV/s, drybox condition. a) Concentration in deposition solution $[ClRh^{III}Pc] = 1.73 \times 10^{-4}$ M b) Concentration in deposition solution $[ClRh^{III}Pc] = 1.15 \times 10^{-5}$ M. The potentials and surface charges of the various peaks are as follows: (peak, V, $\mu C/cm^2$) Ia, 0.02, 6.2; Ib, 0.02, 1.9; IIa, -0.32, 0.44; IIb, -0.32, 0.43.

Figure 4. Cyclic voltammograms for ClRhTNPc (**2**) in 0.1 M KOH, argon degassed. a) equilibrium scan from 0.2 V to -1.2 V b) scan from 0.2 V to -0.2 V after polarising the surface at zero potential for 30 s. c) the first scan following trace (b), from 0.2 V to -0.5 V. d) the second scan after (b) from 0.2 V to -0.5 V.

Figure 5a. Cathodic current of peak **I** and peak **II**, species (**2**), plotted against the scan rates for the surface in Figure 2A. See text for significance of line.

Figure 5b. The total cathodic peak charges for peak **I** and peak **II**, species (**2**), plotted vs. scan rates, for surface in Figure 2A. See text for significance of line. The data are rather scattered due to the difficulty in estimating the residual currents which must be subtracted from the observed data before plotting.

Figure 6. Cyclic voltammograms for ClRhTNPc (**2**) in 0.1 M KOH. a) equilibrium scan from 0.2 V to -1.0 V, argon degassed. b) scan from 0.2 V to -0.2 V for 60 s after about 0.01 mM of dioxygen is introduced in the cell. c) (bottom) the second scan after (b) from 0.2 V to -1.0 V. Scan rate 100 mV/s.

Figure 7A. Cyclic voltammogram for $ClRh^{III}Pc$ (**1**), layer adsorbed from DCE/5% ethanol solution on HOPG electrode, 0.1 M KOH, saturated with dioxygen. Scan rate 100 mV/s.

Figure 7B. Rotating disc electrode study of surface in Figure 7A.
400 rpm, scan rate 20 mV/s.

Table 1 Peak Potentials (Volts vs SCE) of Peak I as a Function of pH.[a]

| pH | Peak I[b] |
|---|---|
| 9.2 | +0.16 |
| 9.75 | +0.11 |
| 9.8 | +0.11 |
| 10.8 | +0.08 |
| 11.4 | +0.09 |
| 12.4 | +0.03 |
| 12.7 | +0.03 |
| 12.8 | +0.02 |
| 12.9 | +0.01 |

a) In general, peak I was very poorly defined at acid pH. b) The average of the anodic and cathodic components is cited. These occurred at the same potential or close thereto. The equations of the best line is:- Peak I E = -0.034(0.003)pH + 0.45(0.01) R = 0.969 for 9 observations. The data in parentheses are standard deviations.

**References**


1) Visiting Professor from the Pharmaceutical Institute, Tohoku University, Sendai 980, Japan.

2) Jahnke, H.; Schonborn, M.; Zimmermann, G. Topics in Current Chemistry **1976**, 61, 133.

3) Tarasevich, M. R.; Radyushkina, K. A. Russ. Chem. Rev., Eng. Trans., **1980**, 49, 1498.

4) van den Brink, F.; Barendrecht, E.;Visscher, W. Rec. Trav. Chim. Pays Bas. **1980**, 99, 253.

5) vanVeen. J. A. R.; van Baar, J. F. Rev. Inorg. Chem. **1982**, 4, 293.

6) Schiffrin, D. J. Electrochemistry **1983**, 8, 126.

7) Yeager, E. Electrochim. Acta **1984**, 29, 1527; Yeager, E. J. Mol. Catal. **1986**, 38, 5.

8) Coowar, F; Contamin, O.; Savy, M.; Scarbeck, G. J. Electroanal. Chem., **1988**, 246, 119.

9) Collman, J. P.; Marrocco, M.; Denisevich, P.; Koval, C.; Anson, F. C. J. Electroanal. Chem. **1979**, 101, 117; Collman, J. P.; Denisevich, P.; Konai, Y.; Marrocco, M.; Koval, C.; Anson, F. C. J. Am. Chem. Soc. **1980**, 102, 6027.

10) Chang, C. K.; Liu, H. Y.; Abdalmuhdi, I. J. Am. Chem. Soc. **1984**, 106, 2725.

11) van der Putten, A.; Elzing, A.;Visscher, W.; Barendrecht, E. J. Chem. Soc., Chem. Comm. **1986**, 477.

12) Collman, J. P.; Kim, A. J. Am. Chem. Soc. **1986**, 108, 7847.

13) Kozawa, A.; Zilionis, V. E.; Brodd, R. J. J. Electrochem. Soc. **1970**, 117, 1470.

14) Kozawa, A.; Zilionis, V. E.; Brodd, R. J. J. Electrochem. Soc. **1971**, 118, 1705.

15) Zagal, J.; Bindra, P.; Yeager, E. J. Electrochem. Soc. **1980**, 127, 1506.

16) Kobayashi, N.; Nishiyama, Y. J. Phys. Chem. **1985**, 89, 1167.

17) Paliteiro, C.; Hamnett, A.; Goodenough, J. J. Electroanal. Chem. **1984**, 160, 359.

18) Ikeda, O.; Itoh, S.; Yoneyama, H. Bull. Chem. Soc. Jpn. **1988**, 61, 1428.

19) Kobayashi, N.; Sudo, K.; Osa, T. Bull. Chem. Soc. Jpn. **1990**, 63, 571.

20) Muenz, X.; Hanack, M. Chem. Ber. **1988**, 121, 235.

21) Berezin, B. D. Dokl. Akad. Nauk. SSSR **1963**, 150, 1039.

22) Keen, I. M.; Malerbi, B. W. J. Inorg. Nucl. Chem. **1965**, 27, 1311.

23) Fu, G.; Fu, Y-S.; Jayaraj, K.; Lever, A. B. P. Inorg.Chem. **1990**, 29, 4090.

24) Manivannan, V.; Persaud, L; Tse, Y-H.; Kobayashi, N.; Lever, A. B. P. paper in preparation.

25) Nevin, W. A; Liu, W ; Lever, A. B. P. Can. J. Chem. **1986**, 65, 855. and references therein.

26) Shigehara, K.; Anson, F. C. J. Phys. Chem. **1982**, 86, 2776.

27) Golovin, M. N.; Seymour, P.; Jayaraj, K.; Fu, Y-S.; Lever, A. B. P. Inorg. Chem., **1990**, 29, 1719.

28) Levich, V. G. "Physicochemical Hydrodynamics", Prentice-Hall: Englewood Cliffs, N.J., **1962**.

29) Kadish, K. M.; Yao, C. L.; Anderson, J. E.; Cocolios, P. Inorg. Chem., **1985**, 24, 4515.

30) Janda, P.; Kobayashi, N.; Auburn, P. R.; Lam, H.; Leznoff, C. C.; Lever, A. B. P. Can. J. Chem. **1989**, 67, 1109.

31) Ni, C-L.; Anson, F. C. Inorg. Chem. **1985**, 25, 4754.

32) Minor, P. C.; Lever, A. B. P. Inorg. Chem. **1983**, 22, 826.

33) Elzing, A.; Van Der Putten, A.; Visscher, W.; Barendrecht, E. J. Electroanal. Chem. **1986**, 200, 313.

34) Gillard, R. D.; Heaton, B. T.; Vaughn, D. H. J. Chem. Soc. A **1970**, 3126.

35) Addison, A. W.; Gillard, R. D. J. Chem. Soc. A **1970**, 2523

36) Ogoshi, H.; Setsune, J.; Yoshida, Z. J. Am. Chem. Soc. **1977**, 99, 3869.

37) Wayland, B. B.; Newman, A. R. J. Am. Chem. Soc. **1979**, 101, 6472; 38) Wayland, B. B.; Newman, A. R. Inorg. Chem. **1981**, 20, 3093.

38) Anderson, J. E.; Yao, C-L.; Kadish, K. M. Inorg. Chem. **1986**, 25, 3224.

Scheme I

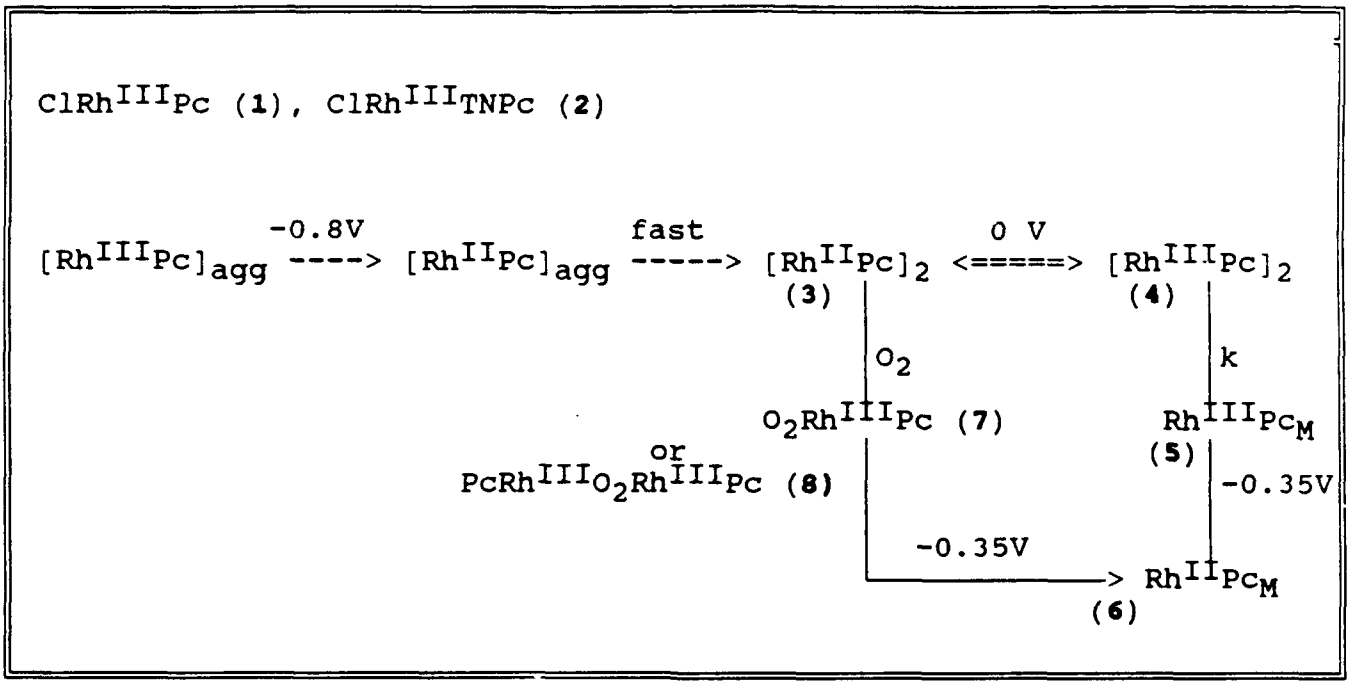
ClRh^III Pc (1), ClRh^III TNPc (2)
[Rh^III Pc]agg
-0.8V
[Rh^II Pc]agg
fast
[Rh^II Pc]2
(3)
0 V
[Rh^III Pc]2
(4)
O2
k
O2Rh^III Pc (7)
Rh^III Pc_M
(5)
or
PcRh^III O2Rh^III Pc (8)
-0.35V
-0.35V
Rh^II Pc_M
(6)

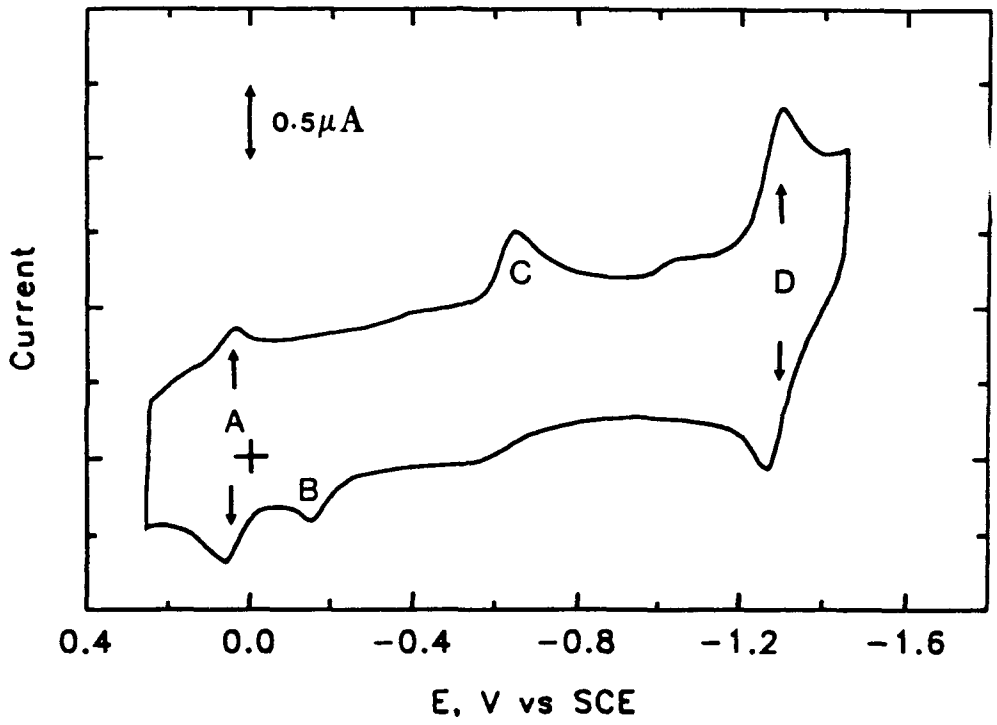
0.5μA
Current
A
B
C
D
0.4
0.0
−0.4
−0.8
−1.2
−1.6
E, V vs SCE

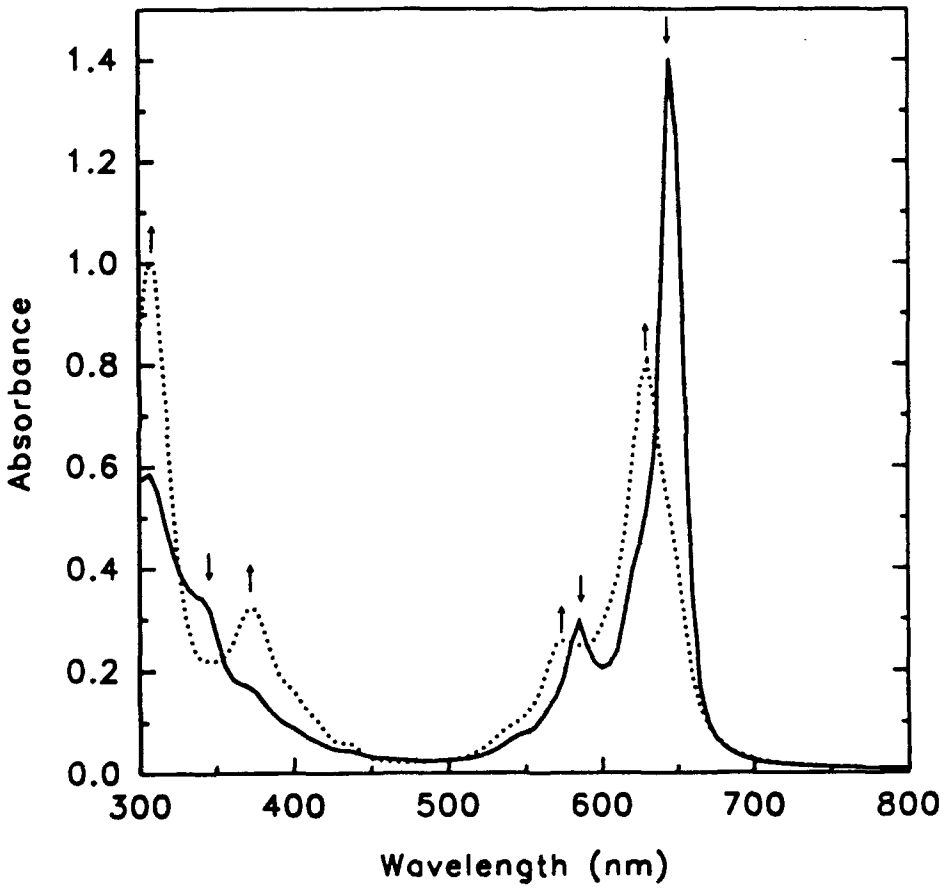
1.4
1.2
1.0
0.8
0.6
0.4
0.2
0.0
Absorbance
300
400
500
600
700
800
Wavelength (nm)

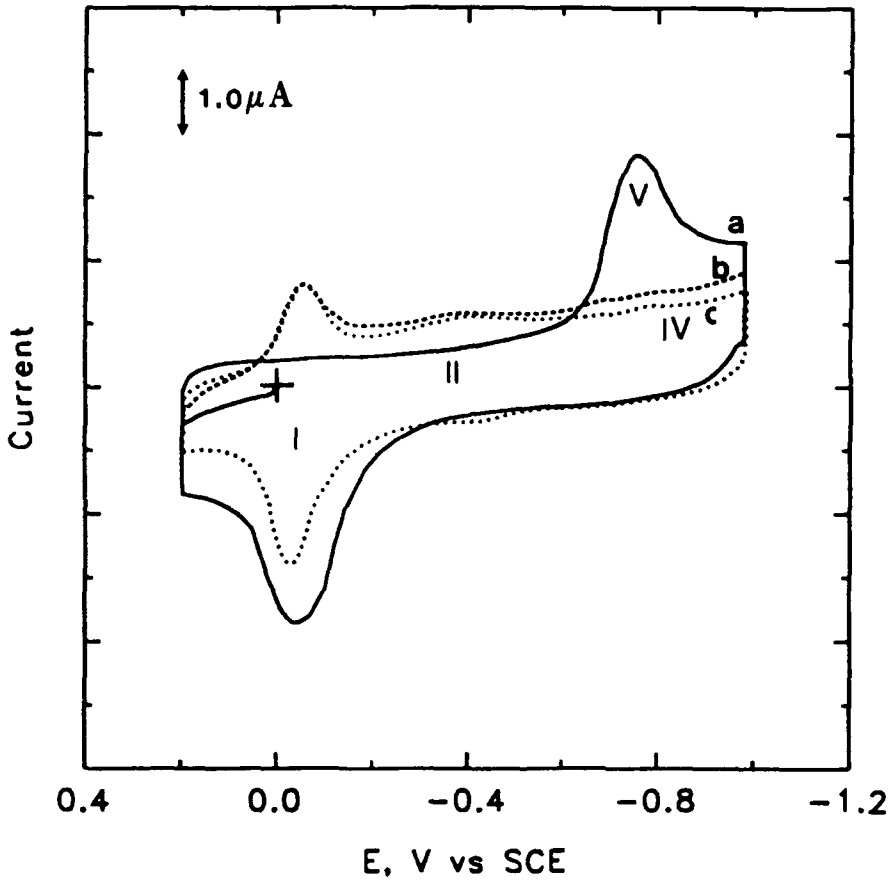
1.0μA
V
a
b
c
IV
II
I
Current
0.4
0.0
−0.4
−0.8
−1.2
E, V vs SCE

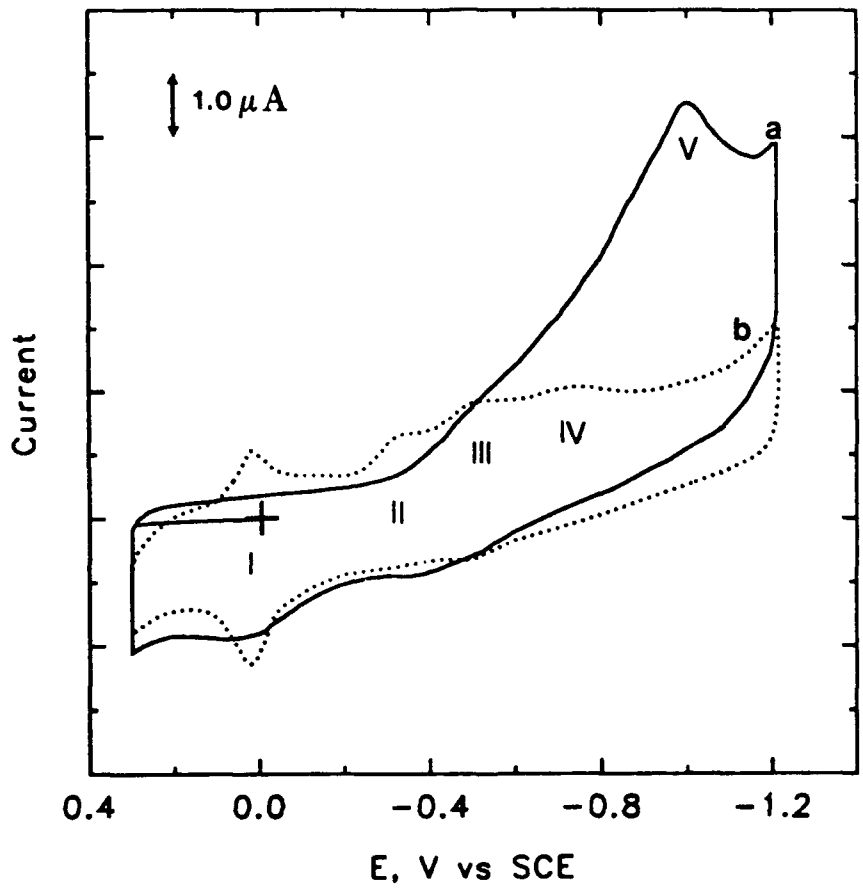
1.0 μA
a
b
V
IV
III
II
I
Current
0.4
0.0
−0.4
−0.8
−1.2
E, V vs SCE

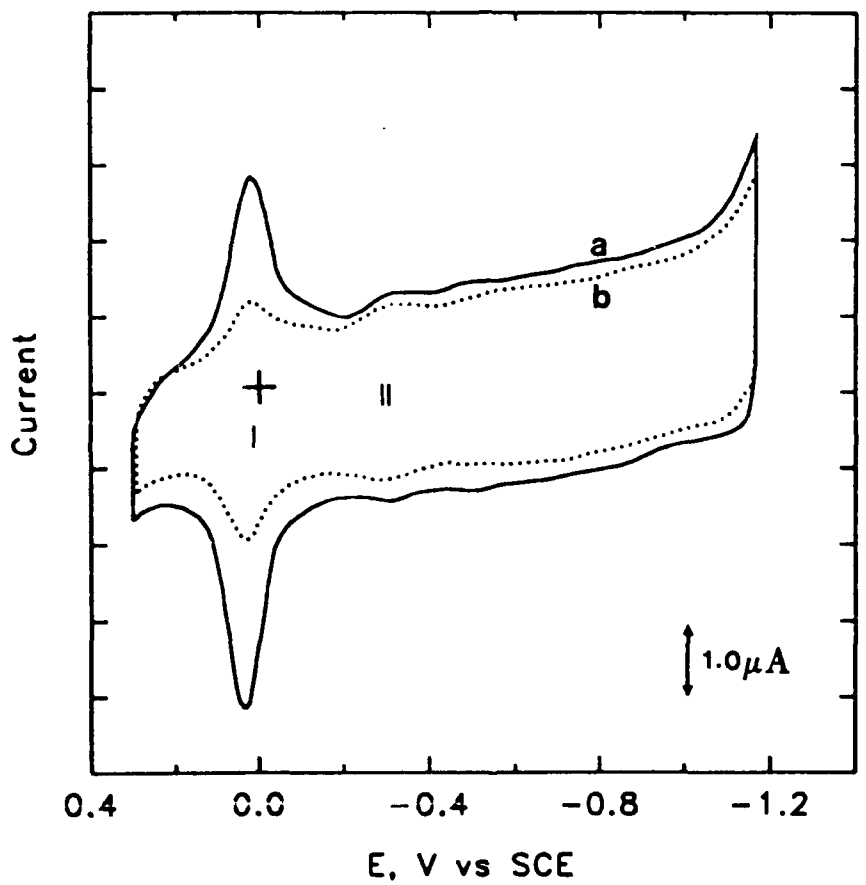
a
b
I
II
1.0μA
Current
0.4
0.0
-0.4
-0.8
-1.2
E, V vs SCE

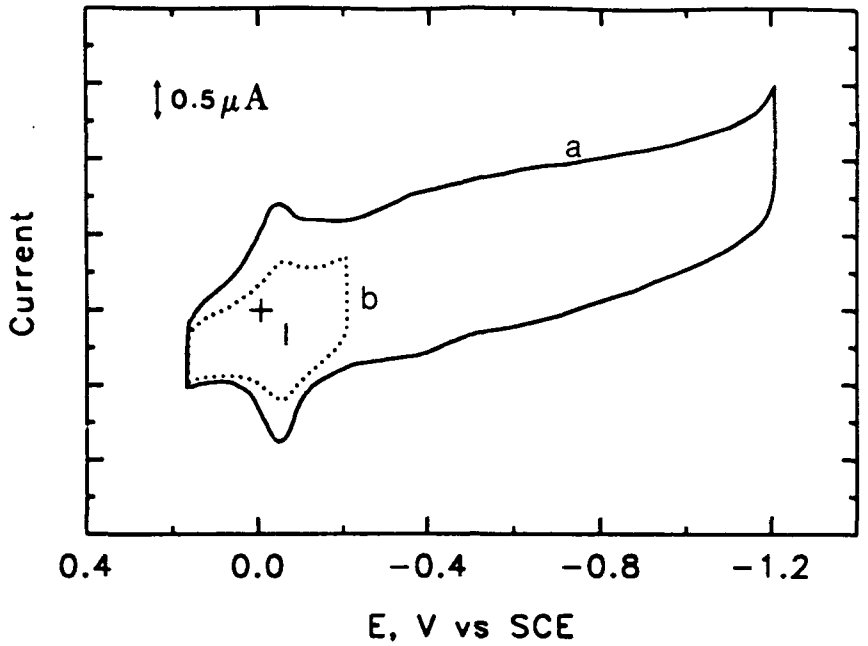
0.5μA
a
b
+
I
Current
0.4
0.0
−0.4
−0.8
−1.2
E, V vs SCE

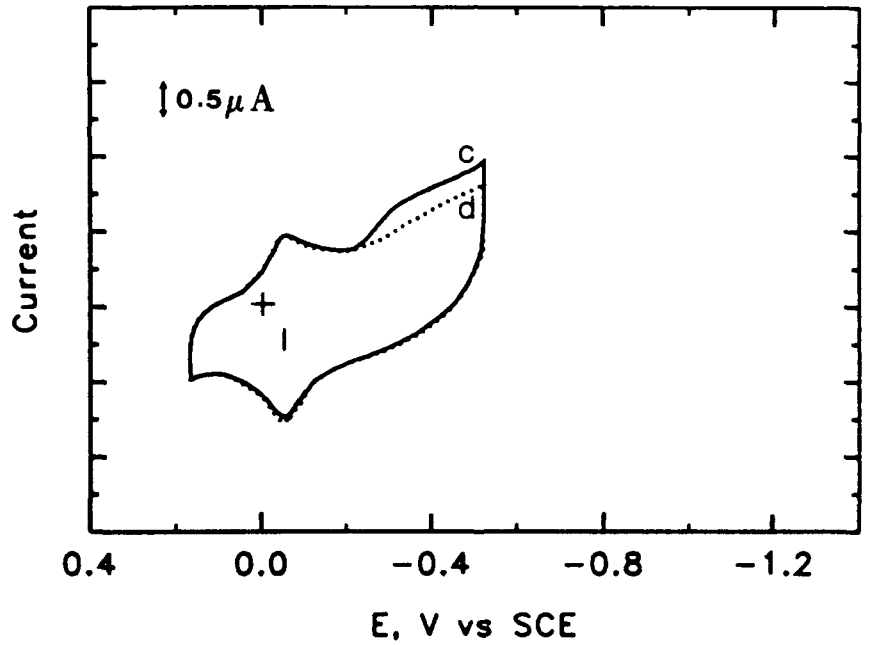
0.5μA
c
d
+
I
Current
0.4
0.0
−0.4
−0.8
−1.2
E, V vs SCE

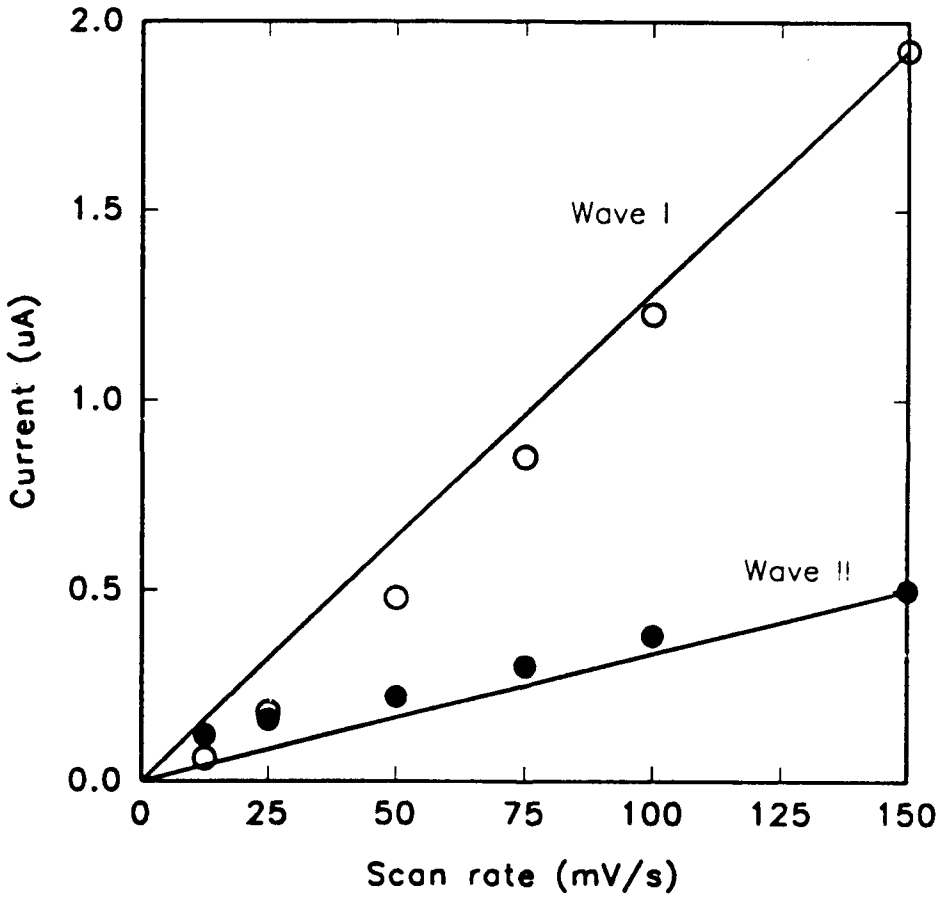
2.0
1.5
1.0
0.5
0.0
Current (uA)
Wave I
Wave II
0
25
50
75
100
125
150
Scan rate (mV/s)

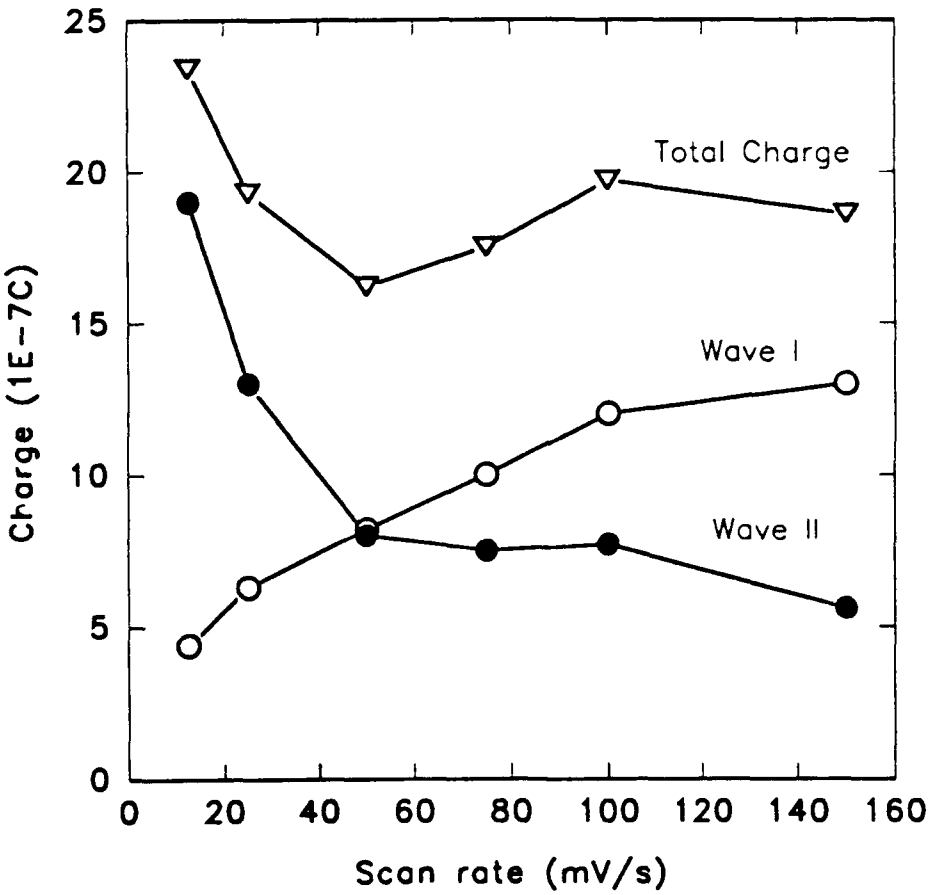
25
20
15
10
5
0
Charge (1E-7C)
0
20
40
60
80
100
120
140
160
Scan rate (mV/s)
Total Charge
Wave I
Wave II

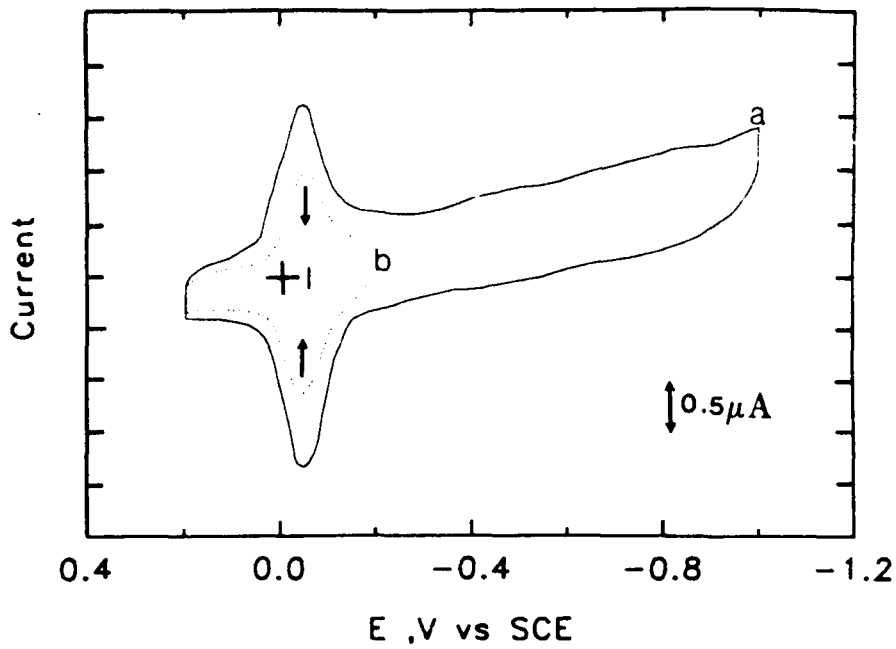
a
b
I
0.5μA
Current
0.4
0.0
−0.4
−0.8
−1.2
E ,V vs SCE

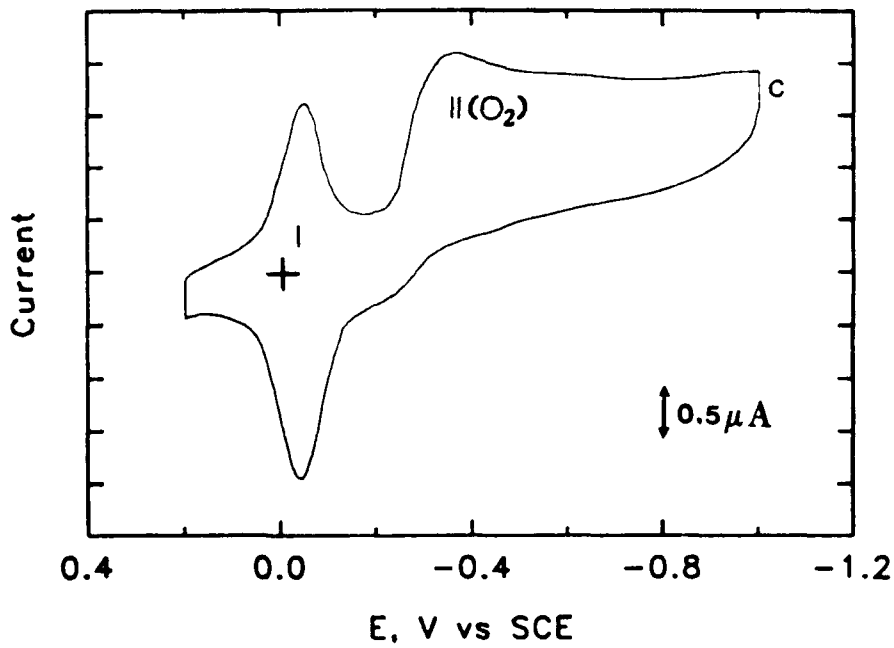
c
II(O2)
I
0.5μA
Current
0.4
0.0
−0.4
−0.8
−1.2
E, V vs SCE

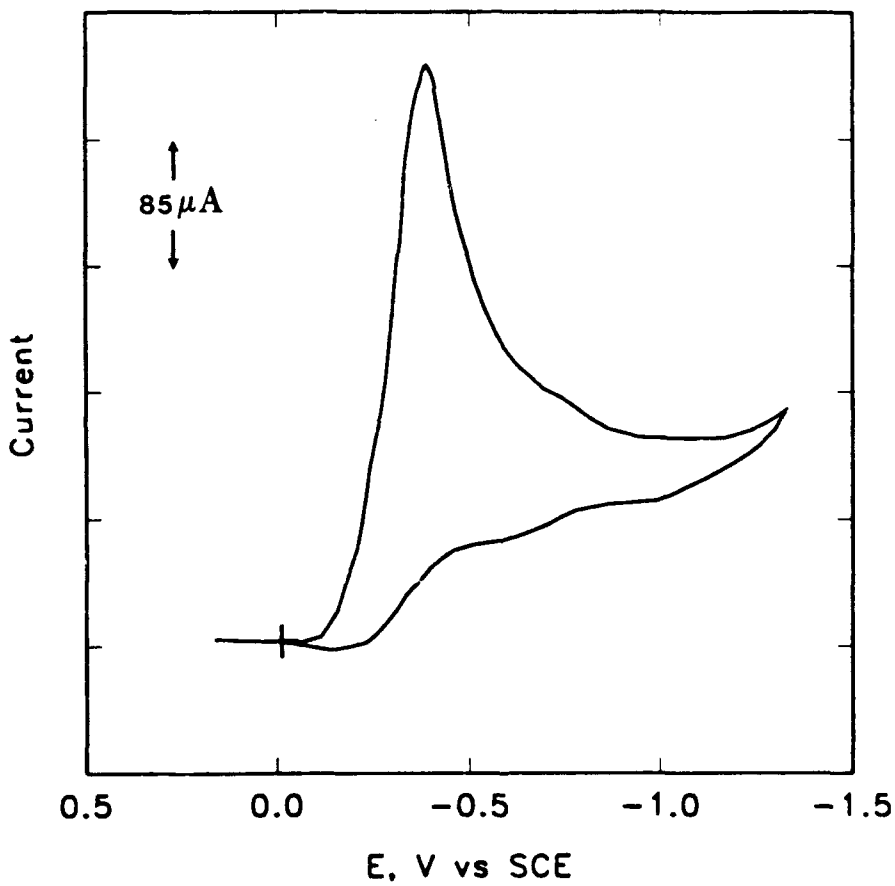
85μA
Current
0.5
0.0
−0.5
−1.0
−1.5
E, V vs SCE

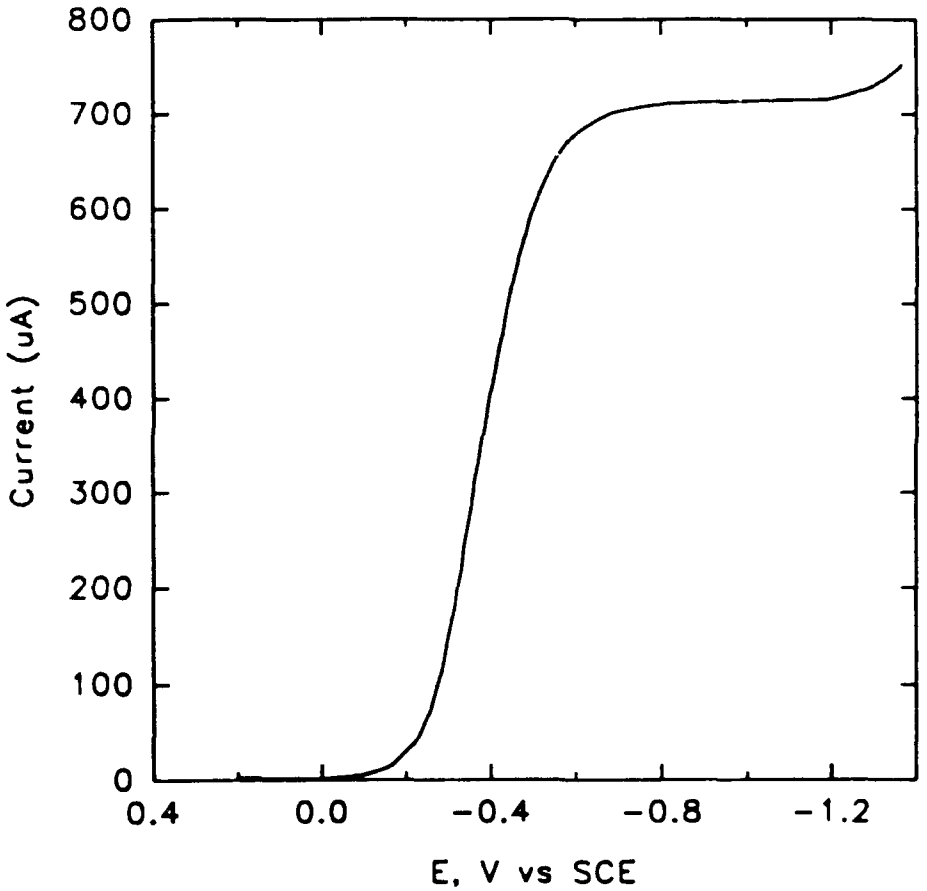
800
700
600
500
400
300
200
100
0
Current (uA)
0.4
0.0
-0.4
-0.8
-1.2
E, V vs SCE